 doi:10.20944/preprints202010.0019.v1

Article

Synthesis of Titanium Dioxide/Silicon Dioxide from Beach Sand as Photocatalyst for Cr and Pb Remediation

Diana Rakhmawaty Eddy [1,*], Soraya Nur Ishmah [1], M. Diki Permana [1] and M. Lutfi Firdaus [2]

[1] Department of Chemistry, Faculty of Mathematics and Sciences, Universitas Padjadjaran, Jl. Raya Bandung-Sumedang km. 21 Jatinangor, Sumedang, Jawa Barat 45363, Indonesia; kimia@unpad.ac.id
[2] Graduate School of Science Education, Bengkulu University, Jl. W.R. Supratman Kandang Limun, Bengkulu 38371, Indonesia; pascapendipa@unib.ac.id
* Correspondence: diana.rahmawati@unpad.ac.id; Tel.: +62-8132-273-1173

Abstract: Heavy metals are non-biodegradable and have a high toxicity effect to living things which makes their presence in the environment extremely dangerous. The method of handling heavy metals waste by photocatalysis techniques using TiO_2/SiO_2 composite showed a good performance in reducing harmful pollutants. In this study, SiO_2 from Bengkulu beach sand was used as a support material for TiO_2 photocatalyst to reduce Cr(VI) and Pb(II) concentrations. SiO_2 was obtained through leaching techniques using NaOH as a solvent. The TiO_2/SiO_2 composite photocatalyst were synthesized using a solvothermal method at 130 °C and then characterized using XRD, FTIR, SEM and PSA. Based on the XRD diffractogram, the synthesized TiO_2 showed the anatase structure while the SiO_2 showed the amorphous structure. Ti-O-Si bond is defined in the IR spectra, which indicates that the relationship between TiO_2 and SiO_2 is a chemical interaction. The results of SEM and PSA characterizations show agglomerated spherical (round) particles with a mean particle size of 616.9 nm. The TiO_2/SiO_2 composite of 7:1 ratio showed the highest photocatalytic activity after 180 minutes of UV irradiation, with a concentration-decrease percentage of 93.77% and 93.55% for for Cr(VI) and Pb(II), respectively.

Keywords: photocatalyst, TiO_2/SiO_2 composite, solvothermal, silica sand

1. Introduction

The rapid growth of technology and manufacturing results in an increase in waste pollution to the environment. The main contributors to water pollution are industrial waste containing heavy metals [1]. These toxic metals cannot be broken down by microorganisms, and when accumulated in the body cause severe illness and even death [2]. Chromium or Cr is a metal that is commonly found in the environment because it is widely used in large industries such as metal coating, petrochemicals, mining, fertilizer, tanning leather, batteries, pesticides and the paper industry [2]. Chromium commonly comes in two forms, trivalent chromium Cr(III) and hexavalent chromium Cr(VI). Chromium in hexavalent form is 500 times more carcinogenic and very toxic compared to its trivalent form because it penetrates into cell membranes and causes harmful effects. The maximum acceptable environmental threshold values for Cr(III) and Cr(VI) are 5 mg/L and 0.05 mg/L, respectively [1].

Besides chromium, water pollution due to the presence of lead is another global concern. Lead or Pb(II) is among the dangerous contaminants found in industrial waste. This compound causes mutations and is carcinogenic. Pb metal is naturally present in water and because of human activities. This metal enters the waters with rainwater help through Pb crystallization in the air [3].

Several methods for removing heavy metals from the environment have been actively investigated through various techniques such as adsorption, cross-flow microfiltration, precipitation and reverse osmosis [1,2]. However, these methods are relatively expensive and often inefficient when working at low concentrations. The method of photocatalysis using semiconductor material

 doi:10.20944/preprints202010.0019.v1

has the potential to reduce harmful pollutants and is also effective when working at low concentrations. Research conducted by Eddy et al. [4] has succeeded in reducing the concentration of Cr(VI) by a percentage of 94% using the photocatalysis method with TiO_2 photocatalyst doped by gadolinium.

Titanium dioxide (TiO_2) is a semiconductor material widely used as a photocatalyst in the purifying wastewater process because it has many advantages such as high photocatalytic activity, high chemical stability when exposed to acidic and basic compounds, high oxidizing power, low toxicity and easy to obtain [5]. Anatase is a form of photocatalyst claimed to be the best for photocatalytic activity, but its transformation into rutile is a weakness that limits its photocatalytic activity. Several studies have been conducted to overcome this problem by modifying the surface of TiO_2 *and* synthesizing composite catalysts such as TiO_2/SiO_2, TiO_2/ZrO_2, $TiO_2/A1_2O_3/SiO_2$, and $TiO_2/ZrO_2/A1_2O_3$ [6]. Furthermore, the modification of TiO_2 using SiO_2 material to improve photocatalytic activity shows a high thermal stability and mechanical strength, and increases the active side of the photocatalyst surface. Another advantage of TiO_2/SiO_2 mixed oxides is that it inhibits transformation from anatase to rutile [5].

Silica is obtained from both living and non-living natural materials, by synthesis and extraction. Based on the types of natural materials that are non-biological, silica is obtained from sand and coal waste such as flying ash sludge. Eddy et al. [7] extracted silica successfully from Palangkaraya beach sand with a benefit of 91.19% and Munasir et al. [8] extracted silica successfully from Tuban beach sand reaching 98.9% gain. In addition, Ishmah et al. [9] and Firdaus et al. [10] have succeeded in extracting silica from Bengkulu beach sand by 97.3% and 99.5%, respectively. In this research, we evaluated the extraction of silicon dioxide (SiO_2) from beach sand precursors and subsequently composite with titanium dioxide (TiO_2) as a photocatalyst for decreasing the concentrations of Cr(VI) and Pb(II).

2. Results and Discussion

2.1. Characterization of Catalyst

Solvothermal method is widely used for the manufacture of oxides that is usually performed at temperatures below 400 °C. The basic principle of this method is the growth of crystals based on material solubility in solvents under high-pressure conditions. Medium temperature conditions are generally used to increase chemical diffusion while high-pressure results in lesser energy consumption compared to temperature. Calcination temperature in the synthesis process has a significant impact on the TiO_2 crystallinity phase, as it also affects the band gap energy value, which has a significant effect on photocatalytic performance. The anatase TiO_2 phase is the best TiO_2 crystal phase to be used in the photocatalytic process with 3.23 eV band gap energy. Based on research by [11], structures with optimum anatase phases are formed at temperatures of 400-600 °C. At temperatures above 600 °C, i.e. at 700 °C, the anatase structure phase begins to be transformed into rutile and the surface area decreases as well as the photocatalyst activity is drastically weakened [12].

XRD analysis of TiO_2/SiO_2 composites was carried out to determine the characteristics of the TiO_2 formed. The resulting diffractogram showed conformity to ICSD 98-015-5245 for amorphous SiO_2 structures and ICSD 98-017-2916 for TiO_2 anatase structures (tetragonal, space group I41/amd). The synthesized TiO_2 crystal showed a peak pattern similar to the TiO_2 P25 Degussa (standard) with the highest peaks at 2θ = 25.25°, 37.80°, 47.89°, and the twin peaks at 53.91° and 55.91°, which is a characteristic area of the anatase type TiO_2 crystals. Figure 1 shows that the composition of TiO_2:SiO_2 affects the peak intensity and the sharpness of the peak produced, while the higher the content of TiO_2 causes the sharpness of the peak intensity.

Preprints (www.preprints.org) | NOT PEER-REVIEWED | Posted: 1 October 2020 doi:10.20944/preprints202010.0019.v1

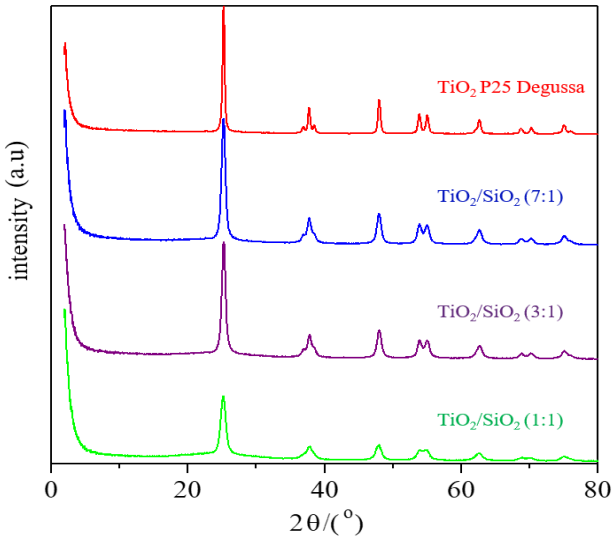

Figure 1. XRD pattern of TiO_2 and TiO_2/SiO_2 composite.

FTIR analysis was carried out to classify functional groups in TiO_2/SiO_2 composites at wave numbers 400-4000 cm^{-1}. The spectrum produced in Figure 2 shows the IR absorption band characteristics at wave numbers 3411-3466 cm^{-1} is -OH stretch vibrations while at 1630-1638 cm^{-1} is a typical absorption for -OH bend vibrations. Calcination on TiO_2/SiO_2 composites can be seen to cause -OH peak absorption to be lower. The strong and dominant absorption peak found in wave number 1099-1102 cm^{-1} is the asymmetrical extension of the Si-O-Si (siloxane) bond. The peak presence at wave 798 cm^{-1} indicates the vibrational strain of the Si-OH bond (silanol) in the amorphous SiO_2 structure. Whereas the absorption peak at wave number 475 cm^{-1} is caused by O-Si-O (siloxy) bonding vibrations. TiO_2/SiO_2 composite formation is characterized by Ti-O-Si bond appearance in the IR spectrum at 940-960 cm^{-1} wavelengths. Ti-O-Si vibrational peak presence indicates that the interaction between TiO_2 and SiO_2 is a chemical reaction process (chemical bonding occurs) rather than a simple physical mixing process. Ti-O-Ti bond appears on wave number 671 cm^{-1}.

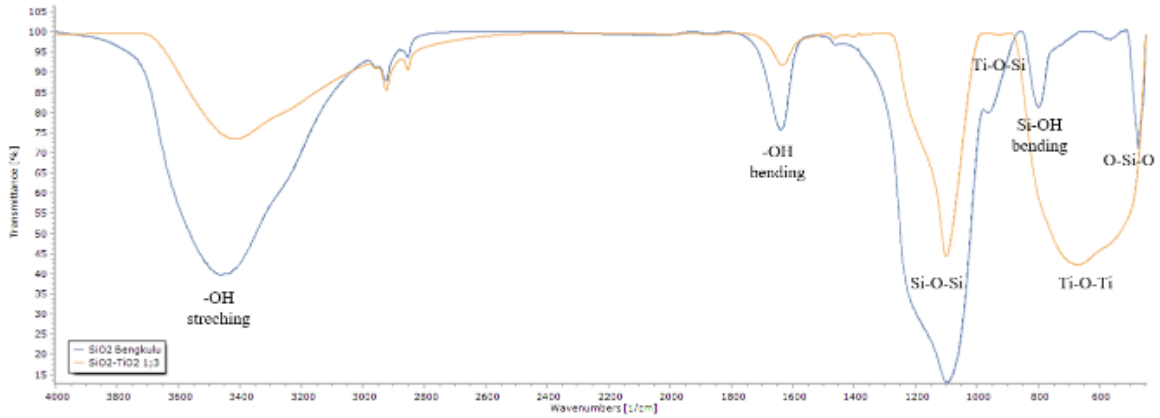

Figure 2. FTIR spectrum of SiO_2 and TiO_2/SiO_2 composite.

SEM analysis is carried out to determine the morphology of TiO_2/SiO_2 composites. Based on the 7000-fold magnification SEM analysis shown in Figure 3, it is known that the TiO_2/SiO_2 composite particles are spherical (round) and agglomeration occurs.

Preprints (www.preprints.org) | NOT PEER-REVIEWED | Posted: 1 October 2020 doi:10.20944/preprints202010.0019.v1

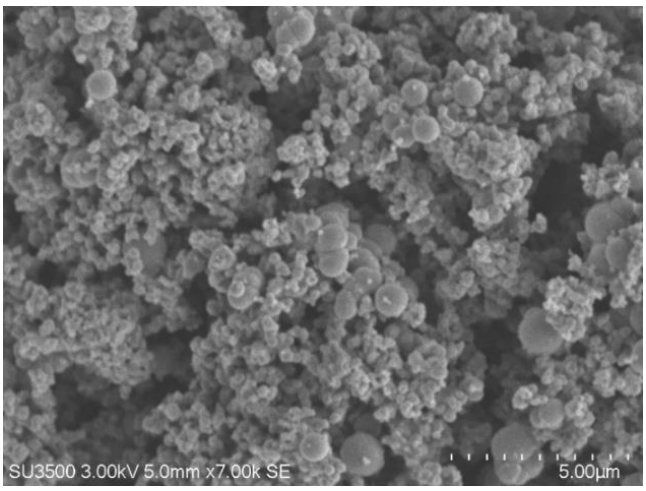

Figure 3. The TiO_2/SiO_2 composite morphology by SEM.

The EDS qualitative analysis is performed to determine the composition of TiO_2/SiO_2 composites. This analysis is based on the X-ray radiation emitted by the atoms in the sample. Figure 4 indicates that the EDS analysis of TiO_2/SiO_2 composites with ratio 3:1, as shown in the sample, elements of titanium (Ti), silicon (Si) and oxygen (O) with atomic percent are 17.94%, 3.43% and 78.62%, respectively.

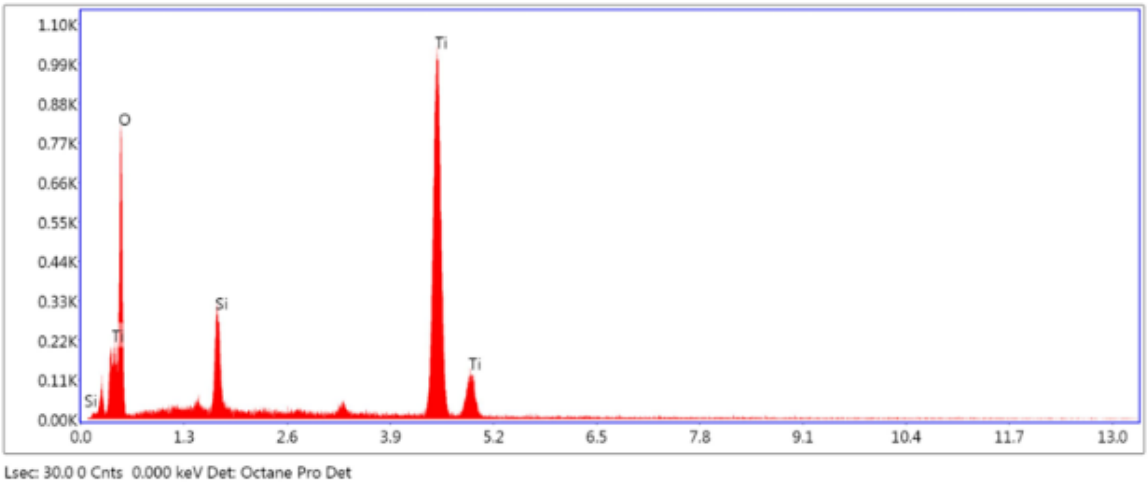

Figure 4. EDS of TiO_2/SiO_2 composite.

The particle size analysis research on TiO_2/SiO_2 composites is carried out to determine the average size and size distribution of the particles. From the data provided in Table 1, it is understood that the more SiO_2 added to the composite, the smaller the average particle size. Z-average values of each composite ratio 1:1; 3:1; and 7:1 respectively 557.4 nm, 616.9 nm and 683.9 nm. Increased number of SiO_2 causes a decrease in agglomeration and therefore reduces the particle size.

Table 1. This is a table. Tables should be placed in the main text near to the first time they are cited.

Particle size	TiO_2/SiO_2 ratio		
	1:1	3:1	7:1
Median (nm)	797.7	628.9	719.0
Mode (nm)	698.5	620.1	696.4
Z-Average (nm)	557.4	616.9	683.9

Decreasing the size of the TiO_2 particle shortens the photoelectron time and the formation of a hole during photocatalytic reactions on the sample surface. It effectively reduces the photoelectron

Preprints (www.preprints.org) | NOT PEER-REVIEWED | Posted: 1 October 2020 doi:10.20944/preprints202010.0019.v1

and hole recombination as well as increases the photoelectron rate and the hole reduction or oxidation which also increases the catalytic photocatalytic performance [6]. The composition of TiO_2 with SiO_2 produces a more even distribution of TiO_2 and a relatively small particle size; therefore, the surface area of TiO_2 is relatively larger and will increase its photocatalytic activity [13]. SiO_2 substrate is an adsorbent that provides an adsorption side that supports TiO_2 through the adsorption process so that more pollutants can be degraded as a remediation procedure [14].

2.2. Photocatalytic Activity

The photocatalyst activity of TiO_2/SiO_2 was tested for decreased concentration of Cr(VI) and Pb(II) metal ions in order to determine the synthesized photocatalyst performance compared to the Degussa TiO_2 P-25. Chromium and lead were chosen as objects because they are examples of heavy metals often found in industrial waste streams. This test was performed using a simulation sample, namely Cr(VI) and Pb(II) ion solution.

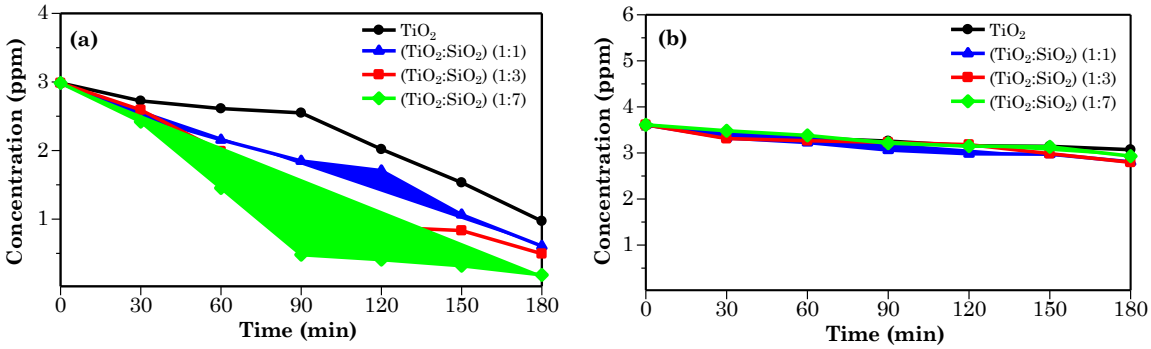

Figure 5. (**a**) Photocatalytic activity and; (**b**) Adsorption activity of catalyst on Cr(VI).

Photocatalytic and adsorption test results of Cr(VI) ions are shown in Figure 5a and 5b. In the same time span, the efficiency of the decreased concentration of Cr(VI) ions in Figure 5a, the UV irradiation sample is greater than the decreased efficiency in Figure 5b without irradiation. It shows that composite powder plays a role as a photocatalytic agent for the reduction of Cr(VI).

Photocatalytic and adsorption test results for Pb(II) ion are shown in Figures 6a and 6b. At the same time, the effect of decreasing the concentration of Pb(II) ions in Figure 6a, with the sample under UV irradiation being greater than the decreasing efficiency in Figure 6b without irradiation, shows that the composite powder plays a role as photocatalytic reducing agent in Pb(II).

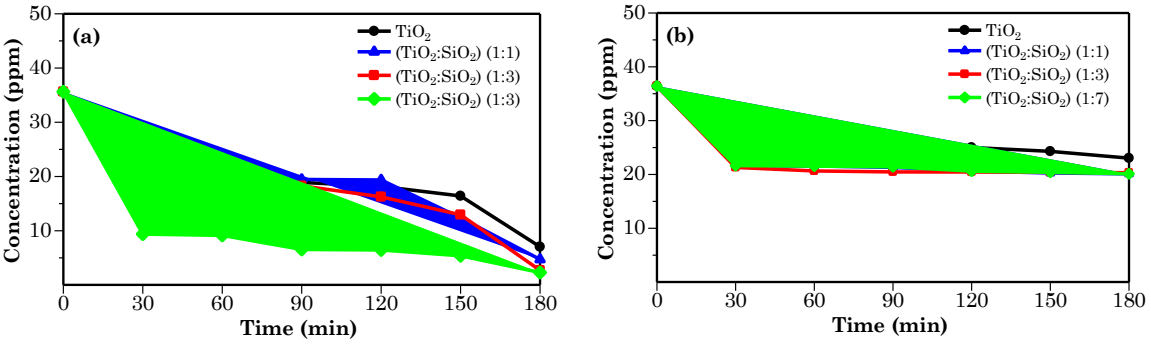

Figure 6. (**a**) Photocatalytic activity and; (**b**) Adsorption activity of catalyst on Pb(II).

Photocatalyst performance exposed to UV rays has a better percentage of reduction compared to photocatalyst not exposed to UV rays. It indicates that photons from UV light determine the performance of photocatalyst in Cr(VI) ions and Pb(II) ions. In photocatalyst exposed to UV light, the photoreduction process begins when photons with more energy than the photocatalyst band gap are absorbed by TiO_2/SiO_2 photocatalyst. Therefore, electron jumps from the valence band to the conduction band and forms a hole in the conduction band (h_{vb}) and the electrons in valence band (e_{cb})

Preprints (www.preprints.org) | NOT PEER-REVIEWED | Posted: 1 October 2020 doi:10.20944/preprints202010.0019.v1

and hole (h_{vb}) will react with oxygen (O_2) and water (H_2O) which are absorbed by photocatalyst then form radicals •OH. Radicals •OH formed then reacts with metals after the process of reduction occurs [15]. Photocatalyst that was not exposed to UV rays (dark conditions), there are no photons that activate the performance of the photocatalyst. Therefore, there was no photoreduction reaction under these conditions. The process that occurs due to a decrease in the concentration of metal Cr(VI) and Pb(II) is a catalytic adsorption process. The adsorption process increases in capacity due to the high content of silica in photocatalyst, because silica is a good adsorbent with a high adsorption capacity.

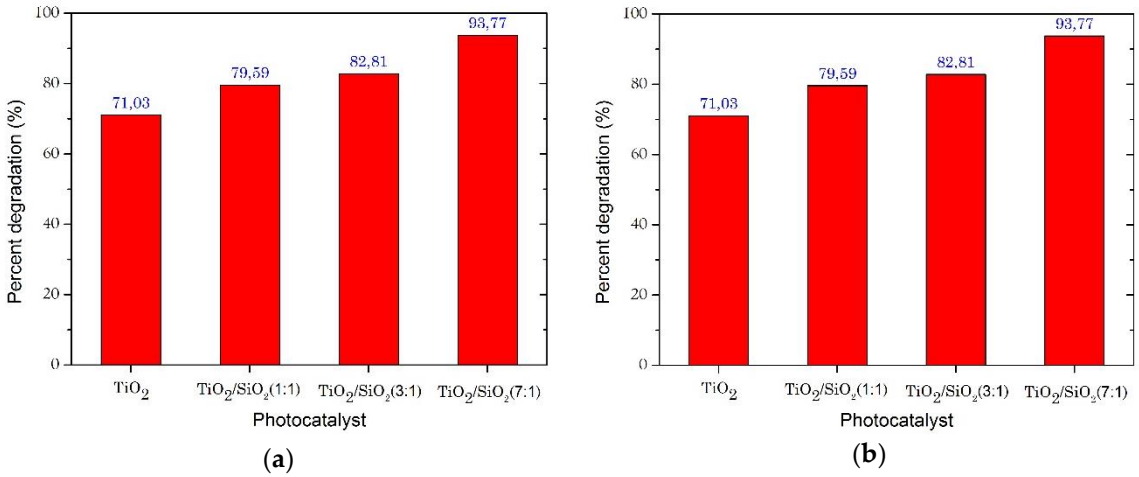

Figure 7. (**a**) Efficiency of decreasing Cr(VI) and; (**b**) Pb(II) concentrations after UV irradiation for 180 minutes.

The effectiveness of chromium and lead concentrations reduction is shown in Figures 7a and 7b. Photocatalytic activity tests with UV irradiation for Cr(VI) ions using TiO_2 photocatalyst only was 71.03%. While those using TiO_2/SiO_2 composites with ratios of 1:1; 3:1; and 7:1 was 79.59%, 82.81% and 93.77%, respectively. The efficiency of concentration reduction after UV irradiation for Pb(II) ions using TiO_2 photocatalyst only was 80.91% and for TiO_2/SiO_2 composites at 1:1; 3:1; and 7:1 ratio were 86.52%, 92.22% and 93.55%, respectively. Although the 1:1 composite has a lower average particle size than the others, the particle size of this composite ratio is very heterogeneous (it can be seen from the maximum width of the wider PSA histogram) causing faster agglomeration, and therefore interferes with the photocatalysis performance of the reduced metal concentrations.

3. Materials and Methods

3.1. Materials

The beach sand used in this study were from the Bengkulu province, Indonesia. Distilled water was used throughout the experiments. Highest-purity available chemicals used in this study were hydrochloric acid (HCl 37%, Merck), ethanol (C_2H_5OH 99.5%, Merck), potassium dichromate ($K_2Cr_2O_7$ 99%, Merck), sodium hydroxide (NaOH 98%, Merck), lead(II) nitrate ($Pb(NO_3)_2$ 99.9%, Merck), titanium dioxide (TiO_2, P25 Degussa, Merck), and titanium tetraisopropoxide (TTIP, $Ti(OC_3H_7)_4$, 97%, Sigma-Aldrich).

3.2. Extraction of Silica

Initially, the beach sand was crushed using ring mill and then sieved with a 325-mesh sieve. In addition, the sand that escaped the sieve was soaked for 12 hours in HCl 2 M and filtered. The resulting residue was then washed with distilled water until no yellowish color is present and then dried at 110 °C. After that, the sandstone was reacted with NaOH 3 M at 95 °C while stirring for 4 hours, and then filtered. The filtrate (sodium silicate) was then stirred and poured drop-by-drop to

 doi:10.20944/preprints202010.0019.v1

form a gel (pH 7) with HCl 6 M addition. The gel formed was stored for 18 hours, and then filtered and rinsed with distilled water and dried at 110 °C. The dried gel was crushed to obtain silica powder.

3.3. The Synthesis of TiO_2/SiO_2 Composite

The TiO_2/SiO_2 composites were synthesized with mole ratio of 1:1; 3:1; and 7:1 (TiO_2:SiO_2). Titanium tetraisopropoxide (TTIP, 520 µL) was prepared and then added to 40 mL of ethanol while stirring to prepare TiO_2/SiO_2 composites with a mole ratio of 3:1. Furthermore, the SiO_2 powder was prepared 0.036 g and sonicated in 20 mL of ethanol for 30 minutes. The SiO_2 suspension was then mixed with the TTIP solution, transferred to an autoclave of 100 mL, and heated in an oven at 130 °C for 15 hours. After cooling until room temperature was achieved, the solution was then centrifuged at 6000 rpm for 10 minutes, and then the pH solution was adjusted to 7.0. The TiO_2/SiO_2 composites formed were then dried at 110 °C for 2 hours and calcinated at 500 °C for 5 hours. Similar procedure was also applied to TiO_2/SiO_2 composites with 1:1 and 7:1 mole ratio variation.

3.4. Characterization of Catalysis

The X-ray diffraction (XRD) diffractogram was carry out using XRD (Rigaku Miniflex 600). Measurement carried out at room temperature using Cu Kα radiation (λ = 1.5406 Å) with scan range from 10° to 80° (2θ). The Fourier Transform Infrared spectra were acquired by a FTIR (Perkin Elmer Spectrum 100) and scan range from 400-4000 cm^{-1}. Particle size of the composites was measured by particle size analyzer (PSA, Horiba SZ-100). Scanning electron microscopy (SEM) was performed by SEM-EDX (Hitachi SU 3500).

3.5. Characterization of Catalysis

The Cr(VI) ion solution was poured to a beaker glass and then added with 100 mg TiO_2/SiO_2 composite with 1:1 ratio. The mixture was then placed on a photoreactor and irradiated with Hg lamps on a magnetic stirrer for 180 minutes. A 10 mL of chromium solution was then taken every 30 minutes using a syringe membrane. The concentration of metal ion was again measured using atomic absorption spectroscopy (AAS, Shimadzu AA 7000). The same treatment was applied to TiO_2/SiO_2 composite with 3:1 and 7:1 ratio, and to TiO_2 without SiO_2 as a control. This photocatalytic activity test was also conducted without irradiation of Hg lamps (for UV irradiation) at the same time interval for each sample. The same photocatalytic activity test procedure was also applied to Pb(II) solution.

4. Conclusions

The composite of SiO_2/TiO_2 increase the photocatalytic activity in decreasing Cr(VI) and Pb(II) concentration. By using the optimum condition, the percentages of heavy metals concentration reduction were 93.77% and 93.55% for Cr(VI) and Pb(II) ions, respectively. The high effectiveness of this method for reducing the concentration of heavy metals can be use as an alternative remediation method of Cr and Pb waste.

Author Contributions: Conceptualization, D.R.E. and M.L.F.; methodology, S.N.I.; software, S.N.I. and M.D.P.; validation, D.R.E. and M.L.F; formal analysis, S.N.I.; investigation, S.N.I. and M.D.P..; resources, S.N.I.; data curation, S.N.I.; writing—original draft preparation, S.N.I.; writing—review and editing, D.R.E. and M.D.P.; visualization, M.D.P.; supervision, D.R.E. and M.L.F.; project administration, D.R.E.; funding acquisition, D.R.E. All authors have read and agreed to the published version of the manuscript.

Funding: This research was funded by Research Grant from Kemenristek-BRIN 2020 with Student Thesis Research Grant Number 1827/UN6.3.1/LT/2020, May 12, 2020.

Acknowledgments: The author thanks to Putri Rizka Lestari and Nobuhiro Kumada from Center for Crystal Science and Technology, University of Yamanashi are acknowledged for characterization analysis.

Conflicts of Interest: The authors declare no conflict of interest.

References

1. Sane, P.; Chaudhari, S.; Nemade, P.; Sontakke, S. Photocatalytic reduction of chromium(VI) using combustion synthesized TiO_2. *J. Environ. Chem. Eng*. **2018**, *6*, 68–73
2. Ojemaye, M.O.; Okoh, O.O.; Okoh, A.I. Performance of $NiFe_2O_4$-SiO_2-TiO_2 Magnetic Photocatalyst for the Effective Photocatalytic Reduction of Cr(VI) in Aqueous Solutions. *J. Nanomater*. **2017**, *2017*, 13.
3. Kotz, J.C.; Treichel, P.M.; Townsend, J.R. *Chemistry and Chemical Reactivity*, 7th ed.; Thomson Brooks/Cole: Australia, 2009.
4. Eddy, D.R.; Rahayu, I.; Hartati, Y.W.; Firdaus, M.L.; Bakti, H.H. Photocatalytic activity of gadolinium doped TiO_2 particles for decreasing heavy metal chromium concentration. *J. Phys. Conf. Ser*. **2018**, *1080*.
5. Besançon, M.; Michelin, L.; Josien, L.; Vidal, L.; Assaker, K.; Bonne, M.; Lebeau, B.; Blin, J.L. Influence of the porous texture of SBA-15 mesoporous silica on the anatase formation in TiO_2-SiO_2 nanocomposites. *New J. Chem*. **2016**, *40*, 4386–4397.
6. Cheng, Y.; Luo, F.; Jiang, Y.; Li, F.; Wei, C. The effect of calcination temperature on the structure and activity of TiO_2/SiO_2 composite catalysts derived from titanium sulfate and fly ash acid sludge. *Colloids Surf. A Physicochem. Eng. Asp*. **2018**, *554*, 81–85.
7. Eddy, D.R.; Puri, F.N.; Noviyanti, A.R. Synthesis and Photocatalytic Activity of Silica-based Sand Quartz as the Supporting TiO_2 Photocatalyst. *Procedia Chem*. **2015**, *17*, 55–58.
8. Munasir; Sulton, A.; Triwikantoro; Zainuri, M.; Darminto. Synthesis of silica nanopowder produced from Indonesian natural sand via alkalifussion route. *AIP Conf. Proc*. **2013**, *1555*, 28–31.
9. Ishmah, S.N.; Permana, M.D.; Firdaus, M.L.; Eddy, D.R. Extraction of Silica from Bengkulu Beach Sand using Alkali Fusion Method. *PENDIPA J. Sci. Edu*. **2020**, *4*, 1–5.
10. Firdaus, M.L.; Madina, F.E.; Yulia, F.S.; Elvia, R.; Soraya, N.I.; Eddy, D.R.; Cid-Andres, A.P. Silica Extraction from Beach Sand for Dyes Removal: Isotherms, Kinetics and Thermodynamics. *Rasayan J. Chem*. **2020**, *13*, 249–254.
11. Zhang, Y.; Weidenkaff, A.; Reller, A. Mesoporous Structure and Phase Transition of Nanosrystalline TiO_2. *Mater Lett*. **2002**, *54*, 375-381.
12. Sikong, L.; Damchan, J.; Kooptarnond, K.; Niyomwas, S. Effect of doped SiO_2 and calcinations temperature on phase transformation of TiO_2 photocatalyst prepared by sol-gel method. *Songklanakarin J. Sci. Tech*nol. **2008**, *30*, 385–391.
13. Sirimahachai, U.; Ndiege, N.; Chandrasekharan, R.; Wongnawa, S.; Shannon, M.A. Nanosized TiO_2 particles decorated on SiO_2 spheres: synthesis and photocatalytic activities. *J. Sol-Gel Sci. Technol*. **2010**, *56*, 3–6.
14. Sellapan, R. *Mechanisms of Enhanced Activity of Model TiO_2/Carbon and TiO_2/Metal Nanocomposite Photocatalysts*. Departement of Applied Physics Chalmers University: Gotebrog, Sweden, 2013.
15. Zaccariello, G.; Moretti, E.; Storaro, L.; Riello, P.; Canton, P.; Gombac, V.; Montini, T.; Rodríguez-Castellón, E.; Benedetti, A. TiO_2-mesoporous silica nanocomposites: Cooperative effect in the photocatalytic degradation of dyes and drugs. *RSC Adv*. **2014**, *4*, 37826–37837.